

# A Composite and Microphysical Study of Jet Stream Cirrus Over the ARM Site

*J. M. Haynes and G. L. Stephens  
Department of Atmospheric Science  
Colorado State University  
Fort Collins, Colorado*

## Introduction

Cirrus are known to play an important role in the radiative budget of the earth-atmosphere system. Previous studies have shown that cirrus within strong jet streams account for about 40% to 60% of all cirrus observed in the continental United States during the winter (Menzel et al. 1992). However, the connection between the properties of mid-latitude cirrus clouds and the large-scale flow that supports them is still, to a large degree, unknown. This study seeks to better quantify and understand this relationship through two interrelated investigations.

First, a composite was performed over fourteen cases of strong jet streams that occurred over the eastern United States, relative to the location of maximum 300-hPa wind within the jet stream. The purpose of this study was to locate areas where cirrus most frequently occur within the jet stream structure. Next, a radar-based retrieval algorithm, set in an optimal estimation framework, was applied to six cases of jet stream cirrus over the Atmospheric Radiation Measurement (ARM) Southern Great Plains (SGP) site. This study detailed the microphysical characteristics of these clouds and the environment, which supported their formation.

## Composite Study

European Center for Medium Range Weather Forecasting (ECMWF) reanalysis data from 1984 through 1987 were scanned for wintertime jet stream events that met the following criteria: (1) the jet stream maximum at 300 hPa occurred in a box over the Eastern United States, in the area favorable for cyclogenesis on the lee side of the Rocky Mountains, (2) the jet stream had predominantly southwesterly flow, and (3) the maximum 300 hPa wind within the jet stream was at least  $70 \text{ m s}^{-1}$ . Roughly 40 events met these criteria, but to ensure independence of samples only the strongest of multiple-day events were selected. This left 14 “key dates” to be composited.

Dynamical data from the ECMWF reanalysis and cloud data from the International Satellite Cloud Climatology Project (ISCCP) DX-level dataset were then composited over a common origin based on the location of maximum wind at 300 hPa for each of the key dates.

The dynamical composite (Figure 1) demonstrates that the composite presents a reasonable semblance to the known structure of mid-latitude cyclones. The dynamical composite features a surface cyclone and cold front, realistic patterns of vorticity advection and vertical motion, and a westward tilt with height.

The cloud composite (Figure 2) similarly demonstrates the success of the composite. The cloud composite features a frontal cloud band, baroclinic leaf structure, and cloud-free region in advance of the surface cold front. A correction (as described in the ISCCP technical documentation) was applied to the base assumption that all clouds emit as black bodies, to account for thin cirrus that are likely to have an emissivity of considerably less than unity.

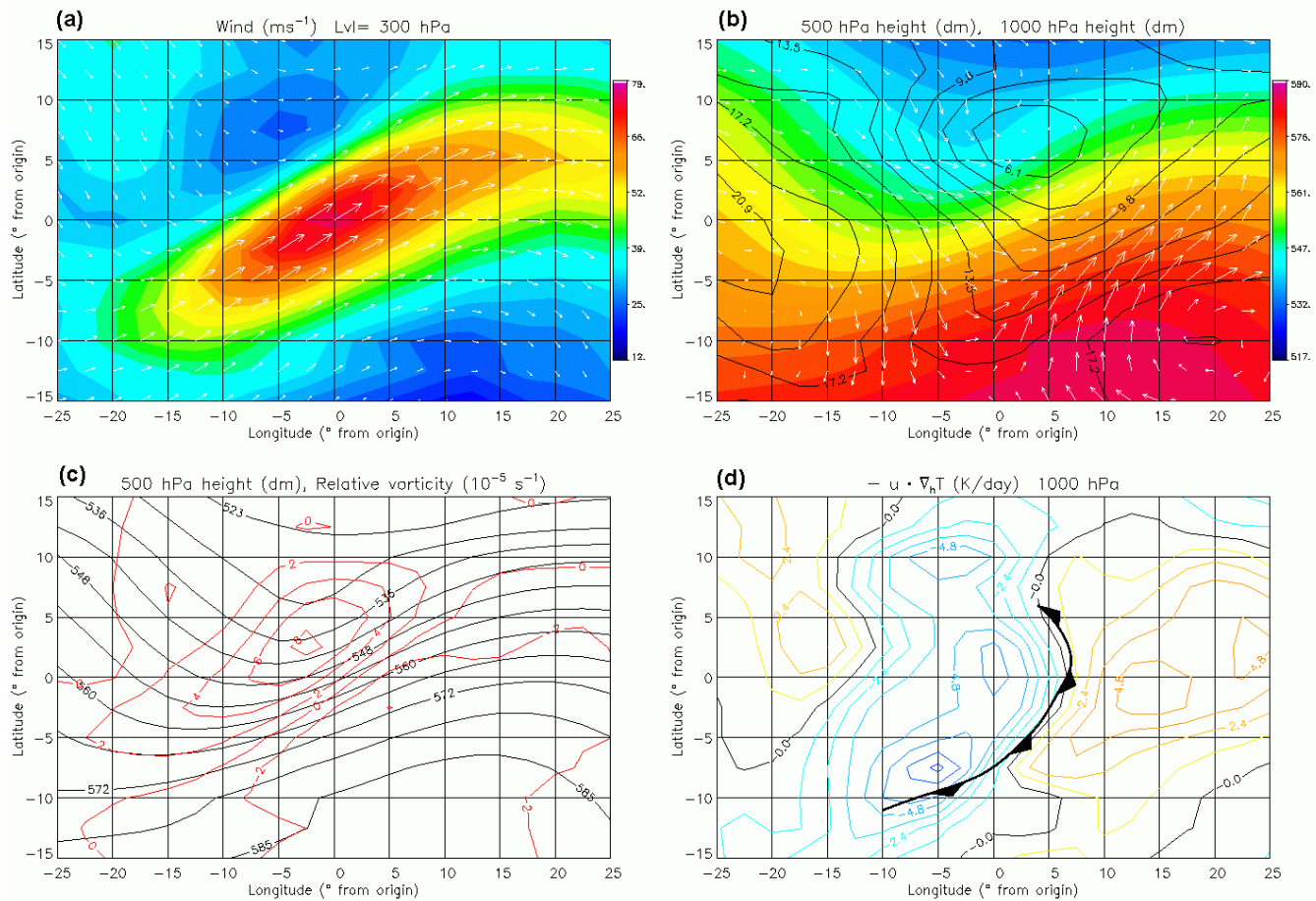


**Figure 1.** Composite dynamical fields: (a) 300 hPa wind, (b) 500 hPa heights (dm) in color, 1000 hPa heights (dm) in black lines, (c) 500 hPa heights (dm) in black and 500 hPa relative vorticity ( $10^5 \text{ s}^{-1}$ ) in red, (d) 1000 hPa temperature advection ( $\text{K day}^{-1}$ ) with composite cold front as determined from pressure field.

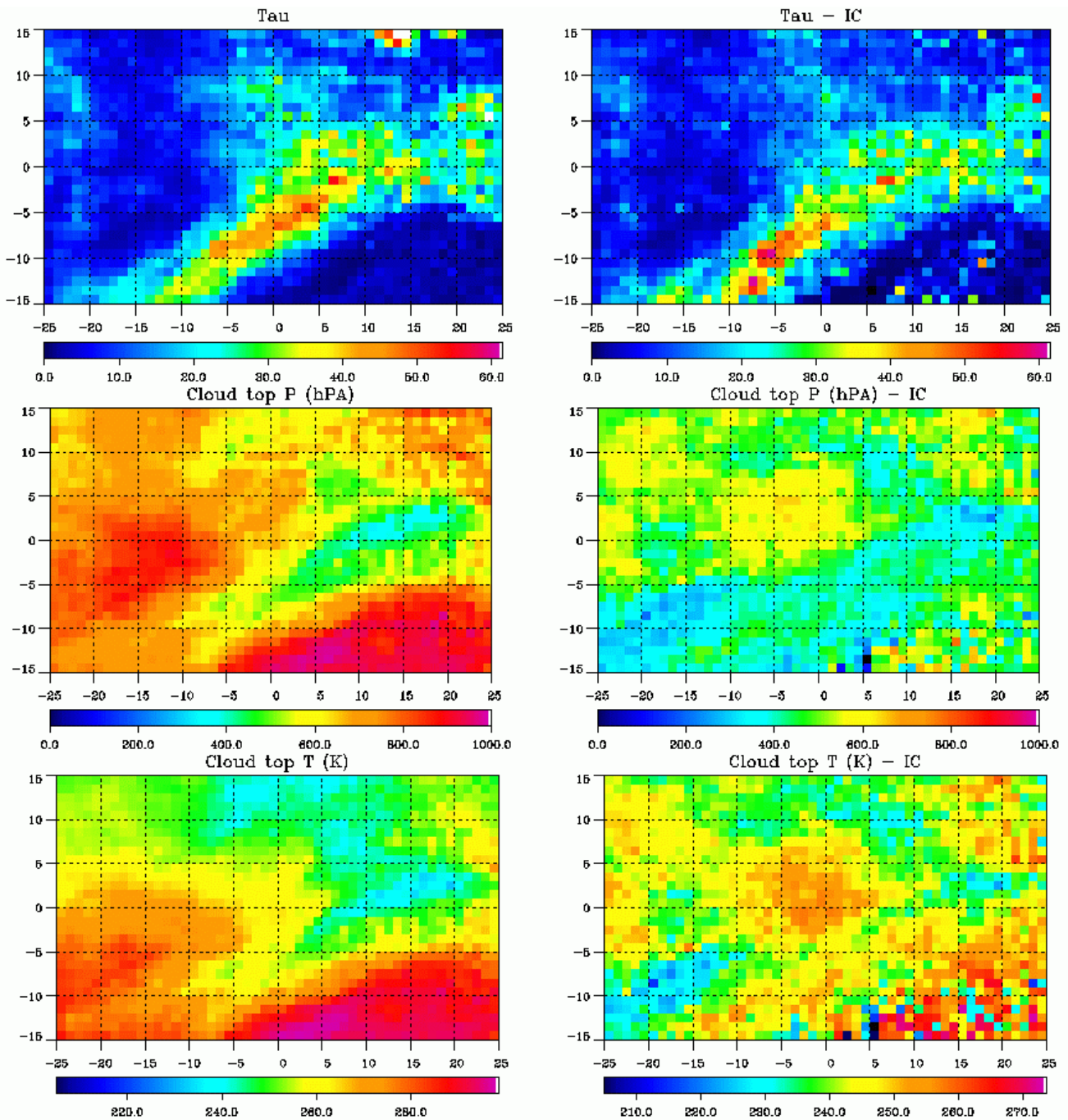


**Figure 2.** Composite visible optical depth (top panel), cloud-top pressure (hPa, middle panel), and cloud-top temperature (K, bottom panel). Left side represents fields derived under blackbody assumption; right side represents fields corrected for the presence of thin ice clouds.

The corrected composite cloud fields were then scanned for pixels where the cloud top temperature and pressure were less than 240 K and 400 hPa, respectively (Figure 3). These were marked as potential cirrus locations and sorted according to optical depth. Cirrus were located primarily in the accelerating

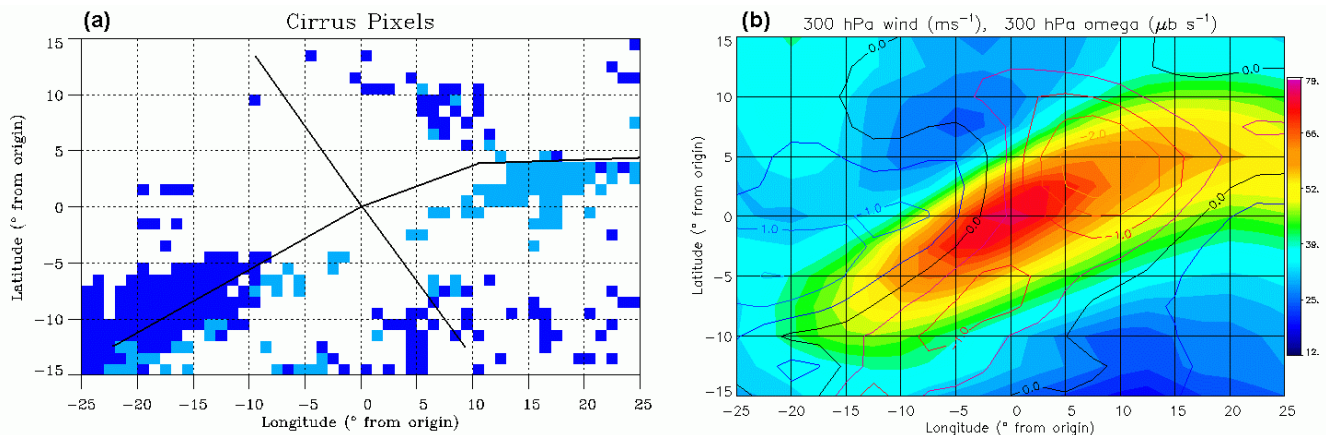


**Figure 3.** (a) Location of cirrus pixels as defined in text. Dark blue indicates optical depth less than 15; light blue indicates optical depth greater than or equal to 15. (b) 300 hPa winds in filled contours and vertical motion ( $\mu\text{b s}^{-1}$ ) in lines.

region of the jet stream, in the area near the comma cloud, and sporadically in the warm sector to the southeast of the jet axis. An area of high, cold clouds with higher optical depths was located in the right-exit region of the jet stream, with a sharp northern boundary against the jet stream axis. Though some convective cloud tops may be present in this region, it is also possible that this is an area of cirrus above lower, thicker clouds in advance of the surface cyclone.

Vertical motion at the level of the jet stream was found to be poorly correlated with the location of cirrus in the composite. With the exception of the comma region, cirrus were located in regions of very weak vertical motion, on the order of  $0.0$  to  $0.05 \text{ Pa s}^{-1}$ , and subsidence was just as common as ascent in the dynamical composite.

## Radar Retrieval Algorithm

A radar retrieval algorithm was applied to six cases of jet stream cirrus that occurred over the ARM site in 1998 and 1999. This algorithm is rather unique in the radar community in that it is posed as an optimal estimation problem. A forward model,  $F$ , was developed that expresses a vector of measurements,  $y$ , in terms of a vector containing parameters to be retrieved,  $x$ :

$$y = F(x, b) + \epsilon_y + \epsilon_F$$

where  $b$  are parameters that affect the retrieval but are not themselves retrieved, and  $\epsilon_y$  and  $\epsilon_F$  are errors in the measurements and forward model, respectively. Direct inversion of the forward model is potentially unstable, so a priori information is used to constrain the retrieval following Rodgers (1976, 1990). Bayes theorem is used to express the most probable state of the atmosphere given the measurements and a priori information, and an iterative solution for  $x$  follows.

The measurements consist of a vertical profile of radar reflectivity from the millimeter wave cloud radar (MMCR) and an estimate of column optical depth derived from the Raman lidar or the multifilter rotating shadowband radiometer (MFRSR). The retrieved parameters consist of a vertical profile of ice crystal size and a column-averaged value of number concentration.

Details on the forward model can be found in an upcoming paper by Benedetti, Haynes, and Stephens. This paper will also discuss algorithm validation. Early validation results are quite favorable and indicate the retrieval scheme is able to retrieve ice water content with an uncertainty on the order of 25% to 50% (Figure 4).

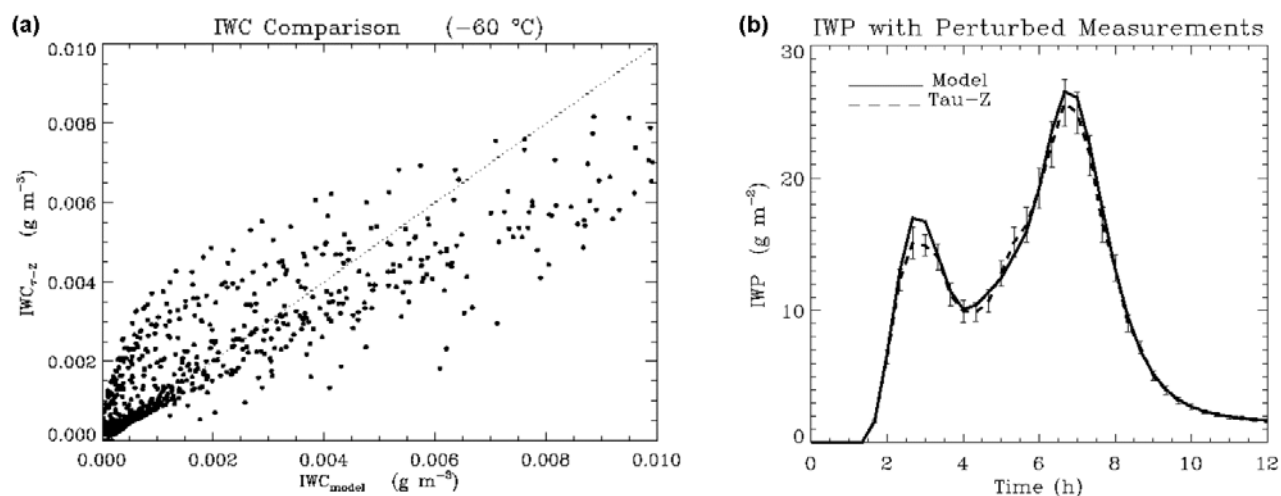


**Figure 4.** (a) Comparison of retrieved ice water content ( $\text{g m}^{-3}$ ) to ice water content from the explicit microphysical model of K. Sassen (University of Utah). (b) Retrieved ice water path ( $\text{g m}^{-2}$ ) compared with modeled ice water path. Results are the means from 40 runs with realistic random noise added to the measurements; error bars show standard deviations.

## Microphysical Study

The results of one of the six case studies, from December 22, 1998, are discussed briefly. A west-southwesterly jet stream with 300 hPa winds exceeding  $70 \text{ m s}^{-1}$  was located over the SGP site. The MMCR reflectivity and Doppler velocity are shown in Figure 5. A cirrus layer was present between 8.5 and 10 km for the first half of the day. Retrieval results from the above algorithm are shown in Figure 6. Ice water content varied from about 0.0 to  $0.08 \text{ g m}^{-3}$ , with an uncertainty of approximately 25%. Ice particle effective diameter varied from about 10 to  $105 \mu\text{m}$  with an uncertainty on the order of 10% to 20%.

Regional dynamics were evaluated using output from the Early ETA model with the accompanying ETA Data Assimilation System (ETA/EDAS). This system incorporates a wide variety of observations into eight daily assimilations, producing a new "initial state" every three hours.

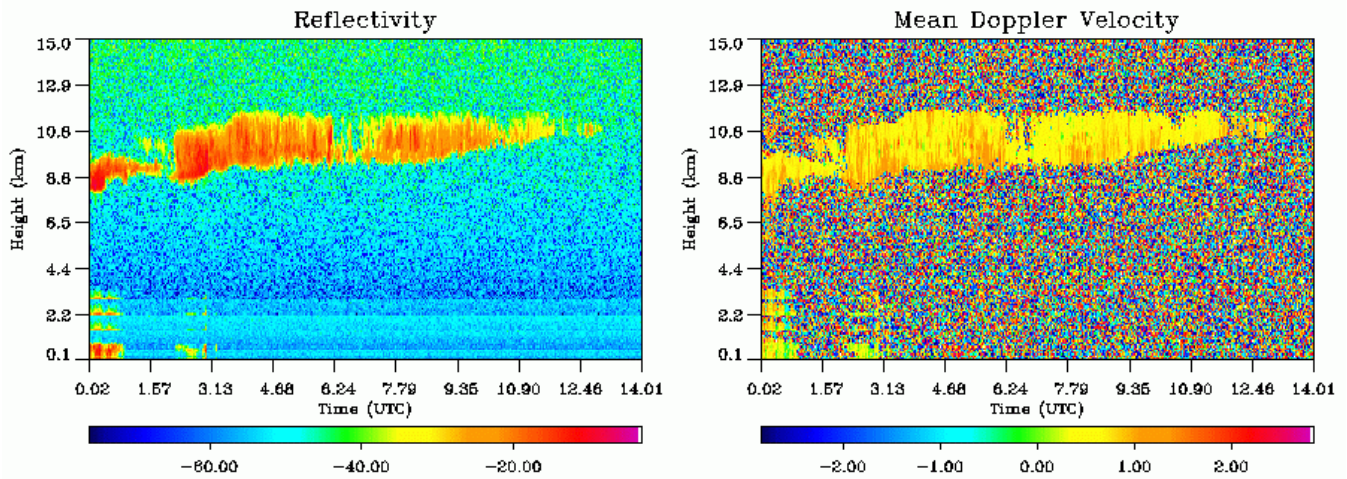


**Figure 5.** MMCR radar reflectivity (dBZ) and Doppler velocity ( $\text{m s}^{-1}$ ) for December 22, 1998.

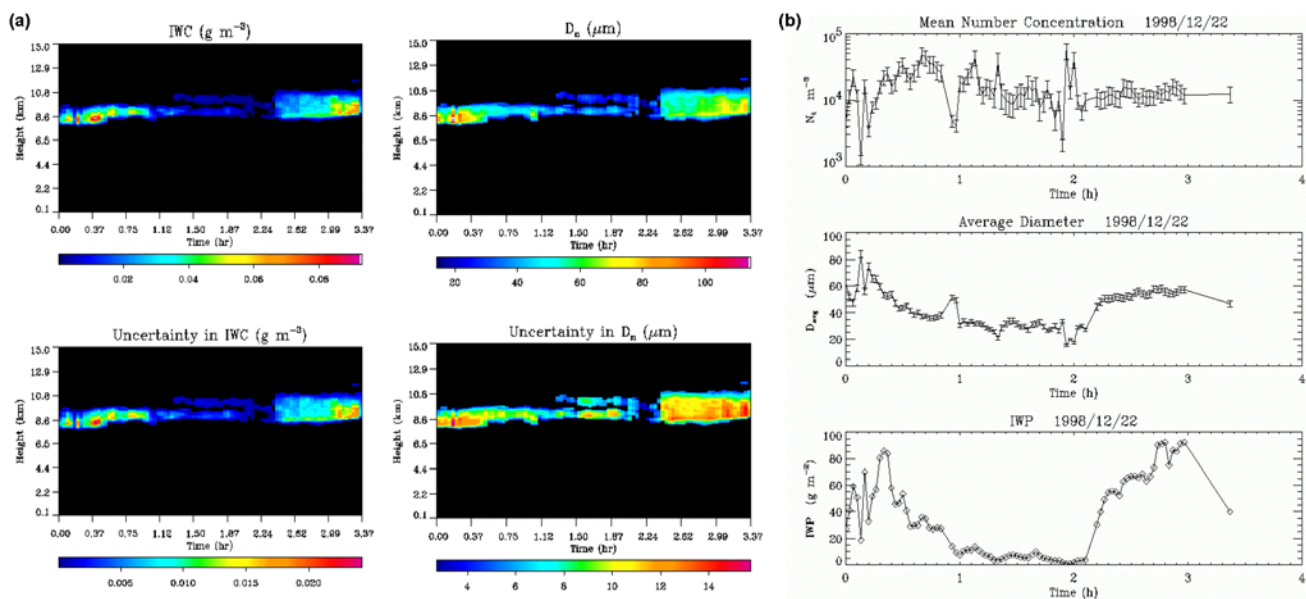


**Figure 6.** (a) Retrieved ice water content ( $\text{g m}^{-3}$ ) and effective particle diameter ( $\mu\text{m}$ ), and associated uncertainties. (b) Column-averaged number concentration ( $\text{m}^{-3}$ ), effective diameter ( $\mu\text{m}$ ), and ice water path ( $\text{g m}^{-2}$ ).

ETA/EDAS output for the time period of interest (Figure 7) reveals that cirrus were diagnosed throughout most of the day. The temporal evolution of this cloud was not well represented by the model, although the cloud height was fairly accurate. In this case and the five others that are not shown here, it was consistently found that vertical motions at cloud level were relatively weak, and often featured significant subsidence. In this case, for example, the only ascending motion diagnosed at cloud level during the first half of the day occurred at the time the cirrus layer was forming. Subsidence on the order of  $0.1$  to  $0.4 \text{ Pa s}^{-1}$  was diagnosed for most of the remaining life of the cirrus layer, and the mean vertical motion over the cloud layer was  $+0.032 \text{ Pa s}^{-1}$  (mean subsidence). This indicates a deficiency in

cirrus representation in the model (Wylie 2002) and may also suggest that other processes, such as horizontal moisture advection, may play a non-trivial role in the formation and maintenance of jet stream cirrus.

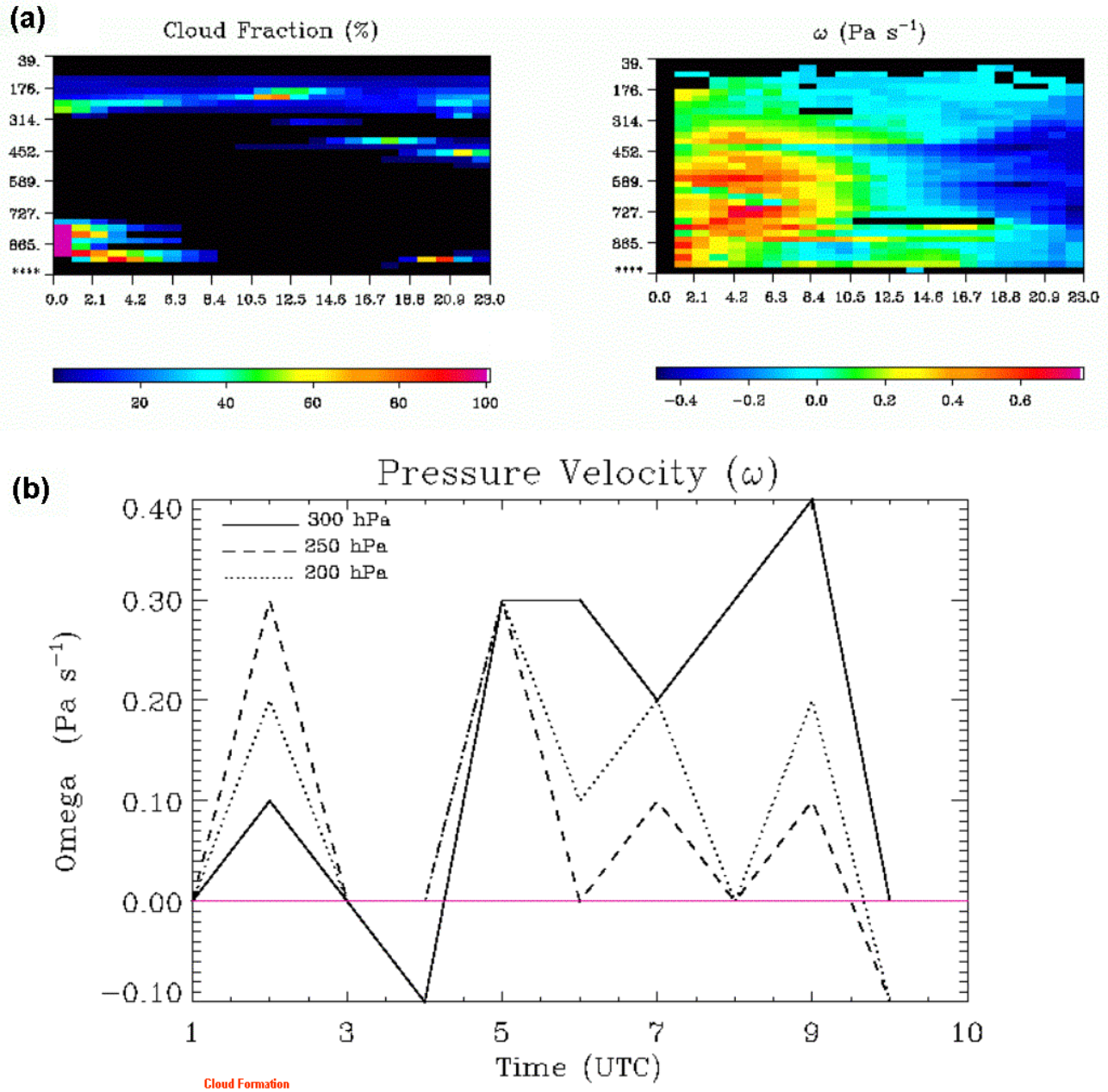


**Figure 7.** (a) ETA/EDAS cloud fraction (%) and vertical motion ( $\text{Pa s}^{-1}$ ). (b) Vertical motion ( $\text{Pa s}^{-1}$ ) at 200, 250, and 300 hPa.

## Summary

- Cirrus were found to occur with greatest frequency in specific regions of the jet stream. They were found to be located primarily in the accelerating region of the jet stream. Other locations where cirrus were persistently located were near the comma cloud, in the right-exit region, and sporadically in the warm sector.
- Cirrus were located in regions of both synoptic scale ascent and subsidence, according to both the composite ECMWF reanalysis data and the ETA/EDAS regional model for the six jet stream cirrus cases over the ARM site.
- These results show a deficiency in model predictions of cirrus and also suggest another process, such as horizontal moisture advection, which may play an important role in cirrus formation and maintenance. This is somewhat counterintuitive given the strong dynamics generally associated with the jet stream.

## References

Menzel, W. P., D. P. Wylie, and K.I. Strabala, 1992: Seasonal and diurnal changes in cirrus clouds as seen in four years of observations with the VAS. *Journal of Applied Meteorology*, **31**, 370-385.

Rodgers, C. D., 1976: Retrieval of atmospheric temperature and composition from remote measurements of thermal radiation. *Reviews of Geophysical and Space Physics*, **14**, 609-624.

Rodgers, C. D., 1990: Characterization and error analysis of profiles retrieved from remote sounding measurements. *Journal of Geophysical Research*, **95**, 5578-5595.

Wylie, D., 2002: *Cirrus and Weather: A Satellite Perspective, in Cirrus*, Eds. D. K. Lynch, K. Sassen, D. Starr, and G. Stephens, Oxford University Press, New York.